Int. J. Electrochem. Sci., 17 **(2022)** Article Number: 220562, doi: 10.20964/2022.05.64

International Journal of
ELECTROCHEMICAL
SCIENCE
www.electrochemsci.org

Electrochemical Sensor Based on Magnetic Molecularly Imprinted Polymer and Graphene-UiO-66 Composite Modified Screen-printed Electrode for Cannabidiol Detection

Xiaosheng Tang[1], *Yong Gu*[1], *Ping Tang*[2,*] *and Liangliang Liu*[3,*]

[1] Hubei Key Laboratory of Edible Wild Plants Conservation and Utilization, National Demonstration Center for Experimental Biology Education, College of Life Sciences, Hubei Normal University, Huangshi, P.R. China, 435002
[2] Hubei Key Laboratory of Mine Environmental Pollution Control and Remediation, School of Environmental Science and Engineering, Hubei Polytechnic University, Huangshi, P.R. China, 435003;
[3] Institute of Bast Fiber Crops, Chinese Academy of Agricultural Sciences, Changsha 410205, China;
[*]E-mail: pingtang@yahoo.com (P. Tang), liuliangliang@caas.cn (L.L. Liu)

Received: 21 February 2022 / *Accepted:* 28 March 2022 / *Published:* 5 April 2022

Cannabidiol (CBD) is a critical compound in *Cannabis sativa* L., having pharmacological effects in treating chronic diseases. To enrich detection methods for *Cannabis sativa* L and related components, we developed an electrochemical sensor to detect CBD. In this research, graphene-UiO-66 composites (Gr-UiO-66) were modified on the screen-printed electrode (SPE) together with magnetic molecularly imprinted polymer (mag-MIP), resulting in a modified sensor marked as mag-MIP/Gr-UiO-66/SPE. The prepared Gr-UiO-66 and mag-MIP were characterized by electron microscope, energy dispersive spectroscopy (EDS), and X-ray powder diffraction (XRD) to confirm the morphology and structure. The fabrication conditions and analytical parameters concerning the composition of modifiers, sequence, concentration, pH, and scan rate were investigated. Under the optimized conditions, the mag-MIP/Gr-UiO-66/SPE exhibited an enhanced electrochemical signal than that in bare electrode, the linear detection from 5 μmol L^{-1} to 100 μmol L^{-1} (r^2 = 0.997), and practicability in real samples. Based on these findings, the utilization of Gr, MOFs, and MIP showed advantages in the fabrication of electrochemical sensors. The proposed mag-MIP/Gr-UiO-66/SPE had the potential to detect natural active compounds in foods, pharmaceutical, cosmetic and health care industries.

Keywords: Cannabidiol; Electrochemical sensor; Graphene; Molecularly imprinted polymer; UiO-66;

1. INTRODUCTION

Cannabidiol (CBD) is becoming popular because of its medical usage in Epidiolex [1]. Unlike the psycho-addictive ingredient Δ^9-Tetrahydrocannabinol (Δ^9-THC), CBD is nonaddictive and exhibited pharmacological functions in the treatments of depression, anxiety, pain, and other chronic symptoms

[2]. As the unique extraction source of CBD, industrial hemp (*Cannabis sativa* L.) is getting more research and plantations in China [3]. As Brighentia *et al.* concluded, gas chromatography-mass spectrometry (GC-MS), high-performance liquid chromatography coupled with diode-array detector (HPLC-DAD), and HPLC-MS were generally available methods for analyzing CBD in labs [4]. However, the rapid detection of CBD is still needed in various scenarios besides laboratory analysis since more and more concerns appeared on analysis of CBD content and cultivation of industrial hemp. Electrochemical sensor is famous for their sensitivity and portability because the size and composition of the sensor could be customized as required [5]. In combination with portable workstations, a rapid detection strategy for CBD would saving much time for farmers and researchers. The screen-printed electrode (SPE) is a kind of versatile sensor, which could be made in various shapes and sizes [6]. With the development in recent decades, SPE has been used to detect trace metals, DNA, food colorants, enzyme activities, estrogens, and other targets with satisfying performances [6-8]. Therefore, designing an electrochemical sensor for CBD using modified SPE is interesting and worthwhile.

Graphene (Gr) is a classical two-dimensional nanomaterial. Due to its distinct advantages in stability, specific surface area, and conductivity, Gr is extensively applied to modify electrodes and has gained popularity [9]. Recently, metal-organic frameworks (MOFs) are a group of tridimensional porous crystalline linked via organic ligands and metal ions, attracting much attention in fabricating electrochemical sensors. It is attributed to the highly ordered polyporous structure and multifunction properties [10]. Among many zirconium MOF, UiO-66 is made by hexameric Zr_6O_{32} units and 2-amino-terephthalate linkers and showed good performances in many fields like adsorption, capacitor, catalysis, medical and environmental detection [11-13].

By binding templates and polymers, molecularly imprinted polymer (MIP) is produced by creating cavities with recognition functions and has advantages in selective separation and enrichment of target molecules [14]. Magnetic MIP (mag-MIP) is a kind of MIP using magnetic nanoparticles as cores and gives traditional MIP the magnetic responsibility. Good enhancement in electrochemical signal and easy separation made mag-MIP appear in the electrode modifications [15].

Till now, reported electrochemical sensors for CBD are limited. Much work could be conducted to develop the detection technology of cannabinoids. Accordingly, many nanomaterials are tried in the modifications of sensors for getting higher electrochemical signals of the target. Gr and UiO-66 are selected as the modifiers, and they are premixed as a kind of composites. Through the ultrasonic treatment of Gr and UiO-66, the forming composites Gr-UiO-66 show a similar enhancing effect and easier fabrication, proved in previous research. Combined with mag-MIP, these modifiers are modified on SPE in sequence resulting in the proposed mag-MIP and Gr-UiO-66 composites modified SPE (mag-MIP/Gr-UiO-66/SPE). The used nanomaterials are well characterized by scanning electron microscopy (SEM), transmission electron microscopy (TEM), and X-ray diffractometer (XRD). The fabrication conditions concerning the composition and sequence of modifiers and the analytical parameters are optimized. The optimized sensor mag-MIP/Gr-UiO-66/SPE exhibits an enhanced electrochemical signal than that in a bare electrode. It also has a good analytical performance and practicability. It could be further developed to detect natural active compounds in foods and health care industries.

2. EXPERIMENTAL

2.1. Chemicals and instrumentation

Graphene (Gr) was purchased from Nanjing XFNANO Materials Tech Co., Ltd. (Nanjing, China). Zirconium chloride, 2-aminoterephthalic acid, N,N-Dimethyl formamide (DMF), and acetonitrile in the chromatographic grade were obtained from Macklin Inc. (Shanghai, China). Cannabidiol (CBD, 99.0 %), Δ^9-Tetrahydrocannabinol (Δ^9-THC, 99.0 %), Cannabidiolic acid (CBDA, 99.0 %) were purchased from Cerilliant as standards (Round Rock, Texas, USA). Sodium acetate, ferric chloride, polyethylene glycol (PEG) 6000, 3-methacryloxypropyltrimethoxysilane (MPS), azodiisobutyronitrile (AIBN), ethyleneglycol dimethacrylate (EGDMA), and methacrylic acid (MAA) were obtained from Sinopharm Chemical Reagent Co., Ltd. (Shanghai, China). 4-Vinylpyridine (4-VP), acrylamide (AM), and acrylic acid (AA) were bought from TCI (Shanghai) Development Co., Ltd. (Shanghai, China). Deionized water used in experiments was obtained by the ELGA water purification system (ELGA Berkefeld, Veolia, Germany). *Cannabis sativa* L. leaves were collected from the experimental base belonging to our research institute, the Chinese academy of agricultural sciences. The sample used for detection was a trial oil product containing 1% (wt%) CBD (Jinnong Co., Ltd, Changsha, China). All other chemicals were analytical grade (Sinopharm, Shanghai, China).

The electrochemical measurements were conducted using a CHI 660E electrochemical workstation (Shanghai Chenhua Co., Ltd., China) equipped with a screen-printed electrode (SPE) were purchased from Qingdao Poten Technology Co., Ltd. (Qingdao, China) composed of a carbon working electrode (4 mm diameter), a carbon auxiliary electrode and an Ag reference electrode. A sensor connector was handmade in the lab adapted for the workstation. The working electrode would be modified in this study as further descriptions.

The morphology of materials was observed by transmission electron microscopy (TEM) on a Tecnai-G20 transmission electron microscope (FEI, Hillsboro, OR, USA), and scanning electron microscope (SEM) on a JSM 6610Lv scanning electron microscopy equipped with an energy dispersive spectroscopy (EDS) detector (JEOL, Tokyo, Japan). The structure of materials was performed by X-ray powder diffraction (XRD) on a RINT 2500 powder X-ray Diffractometer (Rigaku Corporation, Tokyo, Japan). HPLC analysis was completed on the Agilent 1260 HPLC included a quaternary pump, an autosampler, a thermostatic column compartment, and a diode array detector (Agilent Technologies Inc., Santa Clara, CA, USA). An Agilent ZORBAX C18 column was employed (250 × 4.6 mm i.d.; 5 μm, Santa Clara, CA, USA).

2.2. Preparation of Gr-UiO-66 suspension

The UiO-66 was prepared by our previous reported procedures [16]. After the preparation, 6 mg of Gr and 6 mg of UiO-66 were weighted and mixed in 1 mL of water. Then, the mixture was submitted in ultrasonic treatment for 30 min. The resulting homogeneously Gr-UiO-66 suspensions were used right after they were ready.

2.3. Preparation of mag-MIP

3-Methacryloxypropyltrimethoxysilane modified Fe_3O_4 magnetic nanoparticles were synthesized according to our previous report [17]. 0.3 mmol of CBD and 1.8 mmol of MAA were mixed in 30 mL of acetonitrile. They were then incubated in an ice bath for 12 h. Then, 0.50 g of 3-Methacryloxypropyltrimethoxysilane modified Fe_3O_4 magnetic nanoparticles, 5.4 mmol of ethyleneglycol dimethacrylate, and 50 mg of 2,2-azobisisobutyronitrile were mixed in 100 mL of acetonitrile and ultrasonically treated for 30 min. Then two mixtures were combined, degassed, and reacted at 50 °C for 6 h and further at 60 °C for 24 h. Finally, the mag-MIP was separated by a magnet and washed with acetonitrile to remove the reactants. Then it was transferred in methanol solution and refluxed in a Soxhlet extractor for 24 h to remove the template. Finally, the mag-MIP was dried in a vacuum. The magnetic non-imprinted polymer (mag-NIP) was made in the same procedures except that there was no template.

2.4. Adsorption capacity of mag-MIP

The adsorption test was conducted to investigate the specific adsorption ability of mag-MIP [18]. 20 mg of mag-MIP were incubated with 5 mL of sample solution. After 30 min incubation under shaken at 25 °C, the mixture was separated immediately using a magnet. The adsorption of the solution was detected at 220 nm by using a spectrophotometer (UV-2700 Shimadzu, Kyoto, Japan). The concentrations of CBD and other analogs were calculated by standard curves, and their adsorption capacities were calculated by the equation:

$$\text{Adsorption capacity} = (C_0 - C_e) \times V / m \times 100\% \quad (1)$$

Where C_0 is the sample concentration before adsorption, C_e is the sample concentration after adsorption, V is the volume of sample, and m is the mass of absorbent.

2.5. Fabrication of the mag-MIP/Gr-UiO-66/SPE

10 μL of the Gr-UiO-66 suspension in 6.0 mg mL^{-1} were carefully dropped on the surface of the working electrode of SPE marked as Gr-UiO-66/SPE. When the layer on the SPE was dried in the air, 10 μL of the mag-MIP suspension (5.0 mg mL^{-1}) were dropped on the working electrode of Gr-UiO-66/SPE in the same way termed as mag-MIP/Gr-UiO-66/SPE after dried. The mag-MIP/Gr-UiO-66/SPE was stored at 4 °C before detection. To discuss the possible fabrication strategy, 10 μL of the Gr (6.0 mg mL^{-1}), UiO-66 (6.0 mg mL^{-1}), and mag-MIP (5.0 mg mL^{-1}) suspension were directly modified on SPE respectively and marked as Gr/SPE, UiO-66/SPE, and mag-MIP/SPE.

2.6. Electrochemical determination of CBD

The electrochemical measurements using the mag-MIP/Gr-UiO-66/SPE were performed by dropping sample solutions on the surface and covering three electrodes of the modified sensor. The CBD

solution was dissolved in 10% methanol (containing 10 mmol L^{-1} of phosphate buffer solution, pH 7.0). Cyclic voltammetry was used as the testing method. The potential range was set as 0 V to 0.8 V with a scan rate at 0.05 V s^{-1}. All experiments were carried out in three duplicates at 25 ± 2 °C. In the detection of real samples, the CBD product was diluted a thousand times with 10% methanol (containing 10 mmol L^{-1} of phosphate buffer solution, pH 7.0) and submitted for electrochemical detection as previously described.

2.7. Determination of CBD by HPLC method

In the HPLC method, the mobile phase was 75% acetonitrile solution containing 0.1% acetic acid. The analysis was completed in the isocratic elution mode for 30 min at 25 °C [19]. The flow rate was 0.8 mL/min and the detector was set at 220 nm. The content of CBD in samples was calculated with the standard curve obtained by the standards.

3. RESULTS AND DISCUSSION

3.1. Characterizations

3.1.1. Morphology analysis

The morphology of Gr was observed through TEM. In the TEM image in Figure 1a, the Gr expressed semitransparent, sheet-like, and wrinkled structure, which agreed with the previous report [20].

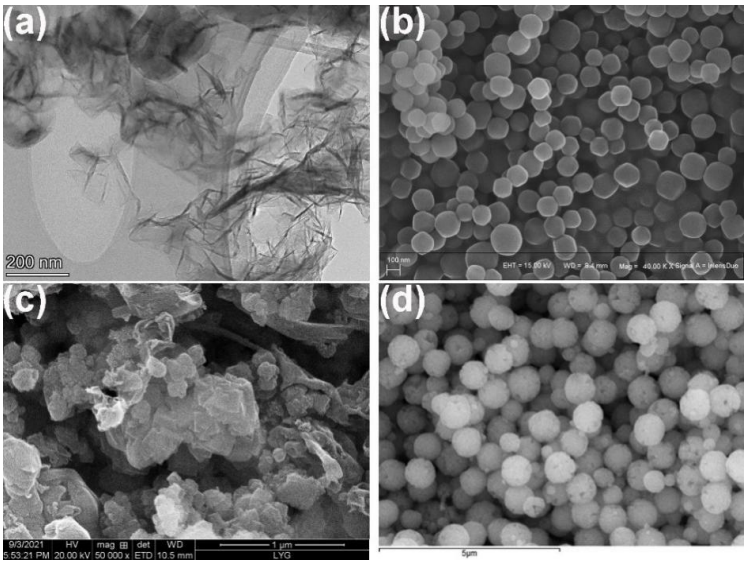

Figure 1. (a) TEM images of Gr; SEM images of (b) UiO-66, (c) Gr-UiO-66 and (d) mag-MIP.

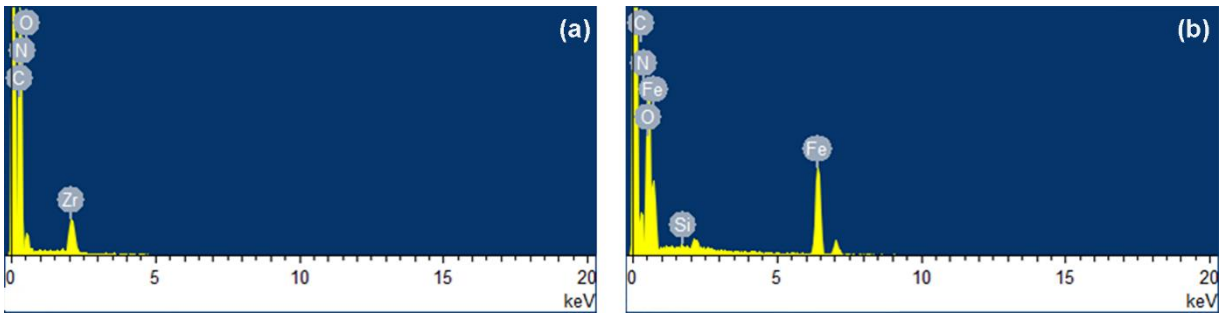

Figure 2. EDS of (a) Gr-UiO-66 and (b) mag-MIP.

The morphologies of UiO-66, Gr-UiO-66, and mag-MIP were investigated by SEM (Figure 1b-1d). The UiO-66 had a polyhedral structure, unlike the mostly reported octahedral structure. It might be because of the small size of prepared UiO-66 [21]. In the SEM image of the Gr-UiO-66 nanocomposites, both particles and silk shapes could be observed. The wrapped particles might indicate the introduction of Gr into the composite. The mag-MIP showed a round sphere shape with a rough surface, similar to previous reports [17,22]. The rough surface might be attributed to the polymerization reaction.

SEM-EDS analysis was further applied to reveal the presence of key elements in Gr-UiO-66 composite and mag-MIP. For Gr-UiO-66 composite, carbon, nitrogen, oxygen, and zirconium elements were analyzed. The EDS diagram showed the proportions of four elements were 33.7at.% of C, 65.8at.% of O, and 0.5at.% of Zr (Figure 2a). The nitrogen was not detected. While, five elements of mag-MIP were investigated in EDS analysis, including carbon, nitrogen, oxygen, iron, and silicon. The EDS diagram of mag-MIP showed their composition was 21.9at.% of C, 1.9at.% of N, 62.4at.% of O, 13.7at.% of Fe, and 0.1at.% of Si, respectively (Figure 2b). The existences of Fe and Si indicated Fe_3O_4 was the core nanoparticles and the following silanization modification.

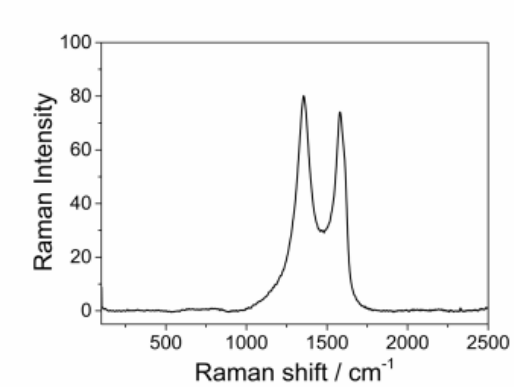

Figure 3. Raman spectrum of Gr.

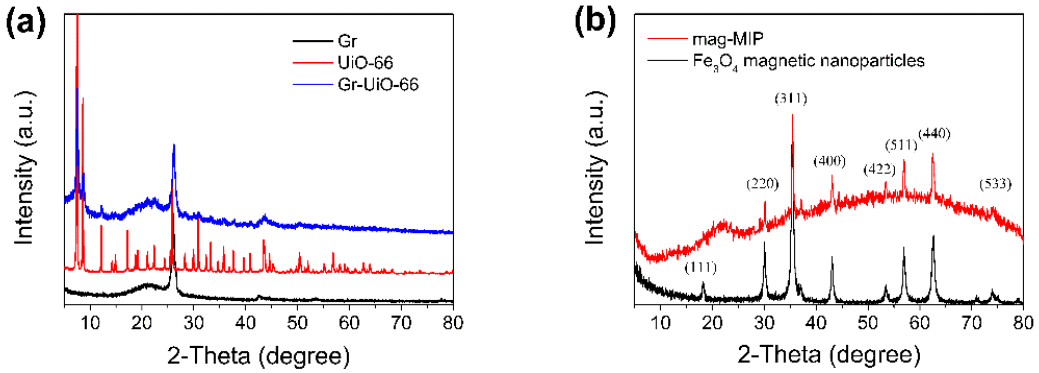

Figure 4. XRD patterns of (a) Gr-UiO-66 and (b) mag-MIP.

3.1.2. Raman

The Raman spectrum of Gr was shown in Figure 3. Gr commonly exhibited D and G bands as references reported [16,19], which corresponded to the sp3 and sp2 structures of carbon. The obtained Gr showed two typical peaks at 1352 cm^{-1} and 1585 cm^{-1}. These two bands agreed with the reported D and G bands, showing the used Gr was eligible.

3.1.3. XRD

The XRD patterns of Gr-UiO-66 composite and mag-MIP were observed and shown in Figure 4 for structural analysis. The prepared UiO-66 showed typical peaks from 5 to 80, which were in accordance with Wang's report [23]. While, in the pattern of Gr-UiO-66 composite, many characteristic peaks could still be found, especially for peaks at 7.53°, 8.74°, and 12.21°. Besides this, the peak at 26.20° could be attributed to the presence of Gr, which could be observed in the pattern of Gr at the same location [24]. However, many detail peaks belonging to UiO-66 were disappeared. It might be because the surrounded Gr in the composites interfered with the signals of UiO-66. Based on these, all the present peaks indicated the existence of Gr and UiO-66 in the composite. On the other hand, the diffraction peaks of mag-MIP were relatively vague. However, the typical peaks belonging to Fe_3O_4 crystal could still be captured in careful observation, which could be confirmed as the indices of Fe_3O_4 nanoparticles including (220), (311), (400), (422), (511), (440), and (533) [25]. These results confirmed that the structures of Gr, UiO-66, and mag-MIP accorded closely with reports.

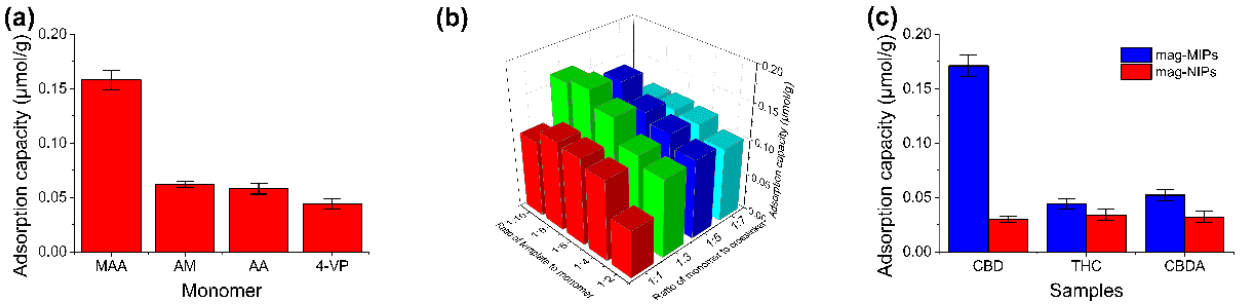

Figure 5. (a) Effect of the monomer on adsorption capacity of mag-MIP; (b) The adsorption capacities of mag-MIP prepared in different mole ratios of CBD to MAA (1:2, 1:4, 1:6, 1:8 and 1:10) and MAA to EGDMA (1:1, 1:3, 1:5 and 1:7); (c) The adsorption capacities of mag-MIP and mag-NIP on CBD, CBDA and Δ^9-THC.

3.2. Optimization and performance of mag-MIP

In order to get a stable mag-MIP, four monomers were compared using the same preparation procedure, and four resulting mag-MIP were tested. As shown in Figure 5a, the adsorption capacities for CBD varied, and the mag-MIP prepared with MAA exhibited the highest value. It could be assumed that better interactions formed between CBD and MAA than other monomers [26]. Hence, MAA was applied as the monomer in the following experiments. The mole ratios of reactants could influence the structure and performance of the resulting mag-MIP. Hence, the effects of mole ratios of CBD to MAA and MAA to EGDMA were all investigated. The adsorption abilities of twenty resulting mag-MIP were illustrated in Figure 5b. As a result, the mag-MIP prepared under the ratio of 1:8:24 showed the optimum adsorption capacity (0.172 μmol/g), which was in accordance with Haupt's report [27]. Therefore, the ratio of 1:8:24 was selected as the optimized mole ratio of CBD: MAA: EGDMA in the preparation.

Figure 6. The images of mag-MIP/Gr-UiO-66/SPE (right) and bare SPE (left).

The specific adsorption abilities of optimized mag-MIP for CBD, Δ^9-THC, and CBDA were investigated. As shown in Figure 5c, the adsorption capacity of CBD was 0.172 μmol/g in mag-MIP, which was 3.9 times that of Δ^9-THC and 3.3 times that of CBDA. The mag-NIP was also tested as a comparison, and the corresponding adsorption capacities of CBD, Δ^9-THC, and CBDA were similar (from 0.03 to 0.034 μmol/g), indicating the adsorption of mag-NIP was unspecific. The mag-MIP had

three times adsorption than analogs and five times mag-NIP, which were better than some reports [18,28]. These data demonstrated the prepared mag-MIP had a specific adsorption ability for CBD.

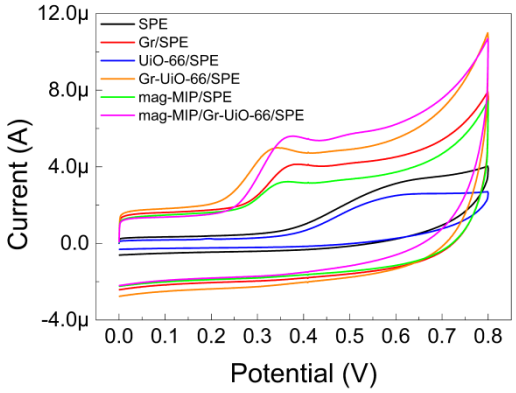

Figure 7. (a) Cyclic voltammetry curves of CBD solution on bare SPE, Gr/SPE, UiO-66/SPE, Gr-UiO-66/SPE, mag-MIP/SPE and mag-MIP/Gr-UiO-66/SPE.

3.3. Electrochemical characteristics of modified electrodes

The electrochemical response of CBD in several modified electrodes was compared. The images of bare SPE and mag-MIP/Gr-UiO-66/SPE were illustrated in Figure 6. It showed the surface of the modified sensor was changed. The cyclic voltammetry curves were illustrated in Figure 7. Through the modifications of Gr, UiO-66, and mag-MIP, the Gr and mag-MIP modified SPE showed an apparent peak at around 0.35 V, which did not exist in bare SPE. The reasons might be the good conductivity and large specific surface area of Gr, the limited conductivity of UiO-66, and the enhanced recognition performance of mag-MIP for target molecules [29-31]. Though the single modification of UiO-66 didn't change the response, the combined modification using Gr-UiO-66 composite exhibited the enhanced effect (2.746 μA). This kind of combination effect between Gr and other nanomaterials appeared in the previous report [17,22]. At last, when the mag-MIP was modified on Gr-UiO-66/SPE, resulting in final mag-MIP/Gr-UiO-66/SPE, its signal (3.929 μA) continued to improve to the Gr-UiO-66/SPE. It showed the advantage of mag-MIP was still playing a role. Therefore, the mag-MIP/Gr-UiO-66/SPE was selected as the optimum composition of a modified sensor for CBD by contributing the best electrochemical signal.

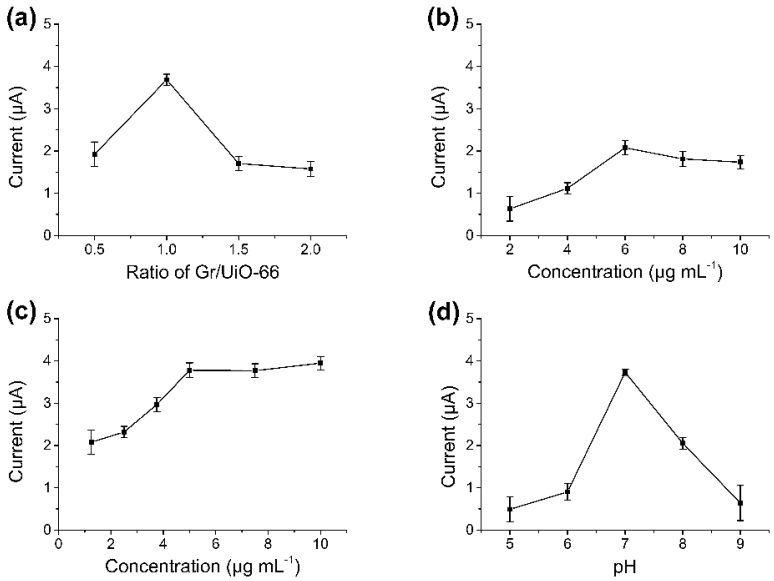

Figure 8. (a) Effect of ratio of Gr to UiO-66 in Gr-UiO-66 on I_p in cyclic voltammetry method; (b) Effect of concentration of Gr-UiO-66 on I_p in cyclic voltammetry method; (c) Effect of concentration of mag-MIP on I_p in cyclic voltammetry method; (d) Effect of pH on I_p in cyclic voltammetry method. The error bars were calculated by triplicate experiments at 25 ± 2 °C.

3.4. Optimization of electrochemical parameters

3.4.1. Composition of Gr-UiO-66

As a composite of Gr-UiO-66, the influence of the mole ratio of Gr and UiO-66 on the electrochemical signals of the resulting sensors was conducted. The change of peak currents with different mole ratios was illustrated in Figure 8a. The concentration of Gr was set according to the ratio to UiO-66, as the UiO-66 was fixed at 6.0 mg mL^{-1}. The graph clearly showed the ratio 1:1 was the optimum ratio of Gr and UiO-66 [17]. Hence, the Gr-UiO-66 composite would be prepared according to the ratio of 1:1.

3.4.2. Concentration

Then the effects of concentrations of modifiers were investigated, including Gr-UiO-66 and mag-MIP. The modification volumes were both fixed at 10.0 μL. Firstly, the impact of concentration of Gr-UiO-66 composite was conducted from 2 to 10 mg mL^{-1} (Figure 8b). 6 mg mL^{-1} of Gr-UiO-66 composite makes the peak current highest, and more materials didn't bring any better results. After that, the effect of concentration of mag-MIP on peak current was conducted from 1 to 10 mg mL^{-1} based on the coating of Gr-UiO-66 (Figure 8c). It could be found that the peak currents reached the maximum when the mag-MIP was higher than 5 mg mL^{-1}. Therefore, the fabrication condition of mag-MIP/Gr-UiO-66/SPE was determined using 6 mg mL^{-1} of Gr-UiO-66 composite and 5 mg mL^{-1} of mag-MIP.

3.4.3. pH

The influence of the pH value of electrolytes on the electrochemical response was further observed. The pH values were verified using buffer solutions. The experiment results shown in Figure 8d showed that the peak current became the highest as the pH value was 7.0. The signals demonstrated decreases in both acidic and alkaline conditions, which might be due to a similar reason as other phenols [19]. Thus, the following experiments were carried out at the electrolyte's optimal pH value (7.0).

3.4.4. Scan rate

The influence of scan rates on the signals of CBD (50 μmol L^{-1}) was studied by the mag-MIP/Gr-UiO-66/SPE. Figure 9a demonstrated the cyclic voltammetry curves and the plots between scan rates and peak currents. The signals increased with the increasing scan rates. And a linear relationship could be observed, which could be seen in the red line in Figure 9b and calculated as Ip = 5.756 v + 2.131 (r^2 =0.986). The linearity indicated this electrochemical process was adsorption-controlled, as many researchers implied [32]. Along with the increasing currents, the signals became more volatile to the growing scan rates. Based on these considerations, the scan rate was set at 0.05 V s^{-1}.

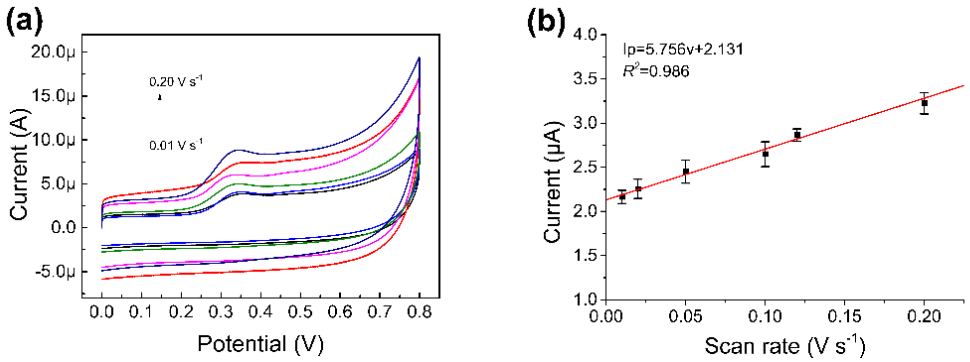

Figure 9. (a) Cyclic voltammetry curves of mag-MIP/Gr-UiO-66/SPE in CBD solution at different scan rates (0.01 to 0.2 V s^{-1}); (b) The Linear graph of I_p and scan rates.

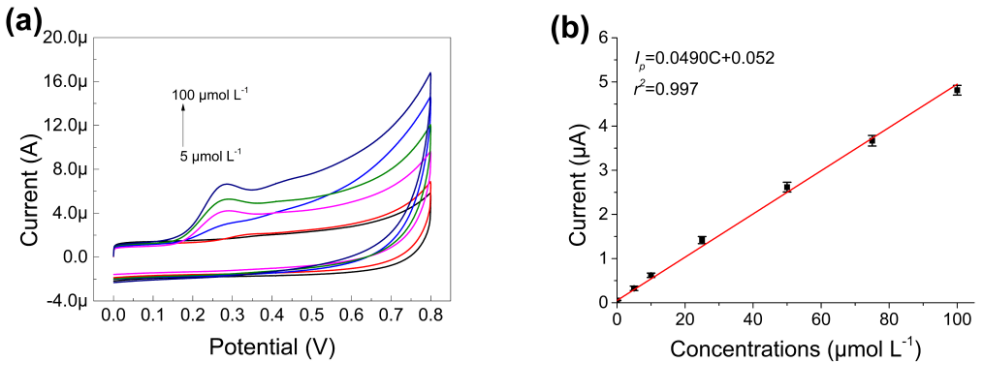

Figure 10. (a) Cyclic voltammetry curves of mag-MIP/Gr-UiO-66/SPE in CBD solution at different concentrations; (b) The Linear graph of I_p and concentration of CBD.

3.5. Quantitative analysis of CBD

The quantitative analysis ability of the mag-MIP/Gr-UiO-66/SPE was evaluated. Various concentrations from 5 μmol L^{-1} to 100 μmol L^{-1} of CBD were detected in cyclic voltammetry. The corresponding cyclic voltammetry curves and plots between concentrations of CBD and peak currents were shown in Figure 10. As a result, a linear dependence at the concentration ranged from 5 μmol L^{-1} to 100 μmol L^{-1} could be found with the detection limit of 0.05 μmol L^{-1} (S/N = 3). The fitted curve was expressed as Ip = 0.0490 C + 0.052 (r^2 = 0.997), which implied the quantitative analysis ability of the mag-MIP/Gr-UiO-66/SPE was acceptable [33-35]. The detection abilities of reported electrochemical sensors for CBD were listed in **Table 1**. Through these researches, the proposed mag-MIP/Gr-UiO-66/SPE showed a wide linearity range, adequate detection ability, and portability based on the usage of SPE. However, the detection limit of the proposed sensor needed further development.

Table 1. Comparison of reported electrochemical sensors for CBD.

Electrode	Linear range (μmol L^{-1})	LOD (μmol L^{-1})	Reference
GC/CB[1]	0.96–6.37	0.35	[36]
Sonogel-Carbon-PEDOT[2]	1.59–19.1	0.94	[37]
NACE–ED[3]	0.32–31.8	0.064	[38]
mag-MIP/Gr-UiO-66/SPE	5–100.0	0.05	This study

[1] GC/CB: Glassy carbon/carbon black.

[2] PEDOT: Poly-(3,4-ethylenedioxythiophene).

[3] NACE–ED: Non-aqueous capillary electrophoresis–Electrochemical detection.

3.6. Anti-interference ability

The anti-interference ability of the mag-MIP/Gr-UiO-66/SPE toward inorganic metal ions and analogs was studied. The concentrations of these interfering inorganic metal ions were 50-fold higher than that of CBD (5.0 mmol L^{-1} to 100 μmol L^{-1}), and the concentrations of CBDA and THC were the same as that of CBD. The ratios of the percent changes in I_p were shown in Figure 11a in the respective additions of Na^+, K^+, Ca^{2+}, Al^{3+}, Cu^{2+}, Mg^{2+}, CBDA, and THC. As a result, the ratios were ranged from 1.07% to 6.49% [39,40]. The Mg^{2+} ion made the most affection during these interferents to the modified sensor.

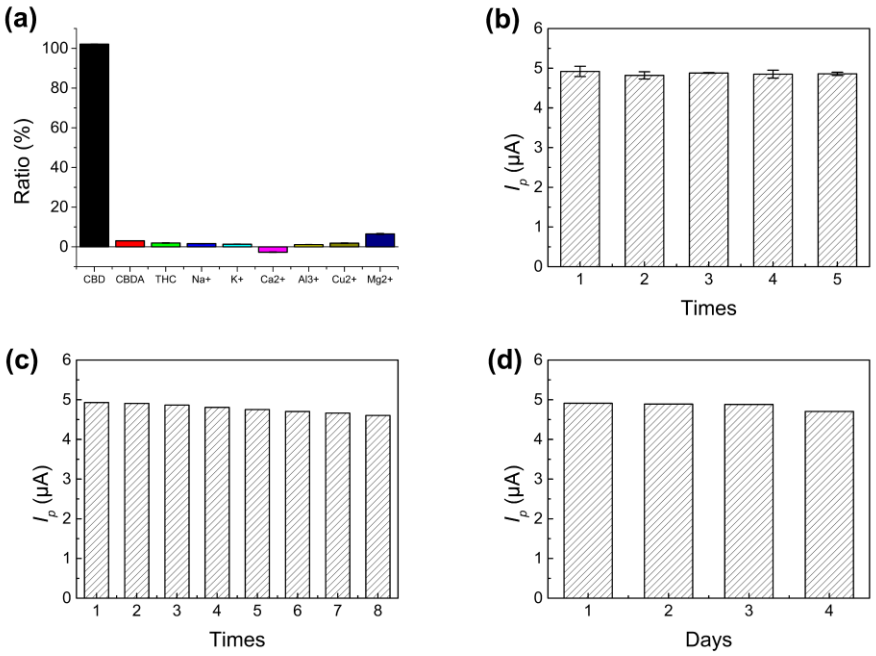

Figure 11. (a) I_p ratios of the mag-MIP/Gr-UiO-66/SPE in CBD solution containing various interfering substances; (b) Reproducibility of the mag-MIP/Gr-UiO-66/SPE in CBD solution; (c) Repeatability of the mag-MIP/Gr-UiO-66/SPE in CBD solution in eight rounds; (d) Stability of the mag-MIP/Gr-UiO-66/SPE in CBD solution in four days.

3.7. Reproducibility, repeatability and stability

The reproducibility of the mag-MIP/Gr-UiO-66/SPE was studied using five independently modified SPE in the same experimental condition for 100 μmol L^{-1} of CBD solution. The calculated relative standard deviation (RSD) value was at 2.13% (Figure 11b). The repeatability of the mag-MIP/Gr-UiO-66/SPE was considered by eight successive detections with the same modified SPE in CBD solution (Figure 11c). The resulting RSD value was at 2.48%. The results showed the mag-MIP/Gr-UiO-66/SPE had satisfactory reproducibility and repeatability in detection [41].

The stability of the mag-MIP/Gr-UiO-66/SPE was checked on four consecutive days. After the fabrication, the electrode was stored at 4 °C at a specific time for detection (Figure 11d). The peak current decreased on the fourth day showing the three days' storage was sufficient for detection. However, more stability research for sensors is still needed in the future because it is closely related to the practicality of sensors.

Table 2. Determination of CBD in real samples. (n = 3).

Samples	Added (μmol L^{-1})	Found (μmol L^{-1})	Recovery (%)	RSD (%)	HPLC (μmol L^{-1})
CBD product	0	31.7	-	1.18	31.9
	1.0	32.6	99.6	1.13	-
	5.0	36.5	99.5	1.35	-
	10.0	41.6	99.8	1.67	-

3.8. Determination of CBD in real samples

The detection in real samples was conducted by the mag-MIP/Gr-UiO-66/SPE. A CBD product was diluted a thousand times with 10% methanol (containing 10 mmol L^{-1} of phosphate buffer solution, pH 7.0) and submitted for electrochemical detection. The standard addition method was applied [42], and the obtained recoveries were between 99.5% and 99.8% (Table 2). The value of the real sample was compared with that in the HPLC method, and the error was 0.2 μmol L^{-1}. During detection, the RSD were under 1.67%. As a result, the electrochemical detection in the real sample using mag-MIP/Gr-UiO-66/SPE was reliable and inconsistent with the traditional method [43].

4. CONCLUSIONS

In this research, mag-MIP was synthesized, and the conditions were optimized. This mag-MIP exhibited good selectivity and adsorption of CBD. Then the Gr-UiO-66 composite and mag-MIP were successively modified on SPE (mag-MIP/Gr-UiO-66/SPE) to form a sensitive electrochemical sensor. The fabrication conditions and analytical parameters of the mag-MIP/Gr-UiO-66/SPE were systematically investigated. As a result, the electrochemical signal of the mag-MIP/Gr-UiO-66/SPE was enhanced. The proposed modified electrode also expressed reasonable practicability and good detection in real samples with good agreement with the traditional method. With satisfying performances in CBD detection, the mag-MIP/Gr-UiO-66/SPE had the potential as a rapid sensor for natural active compounds. Compared to the traditional chromatographic method, electrochemical sensors still had some drawbacks, such as the selectivity in complex samples and the stability or endurance in a long-term monitor. Much work on the modifications and evaluations still needs to be carried out in the future to make the sensors better.

ACKNOWLEDGMENTS
This work was supported by the Open Project Fund of Hubei Key Laboratory of Mine Environmental Pollution Control and Remediation (2017106).

References

1. J. Corroon, R. Kight, *Cannabis Cannabinoid,* 3 (2018) 190-194.
2. K.A. Schoedel, I. Szeto, B. Setnik, E.M. Sellers, N. Levy-Cooperman, C. Mills, T. Etges, K. Sommerville, *Epilepsy Behav.,* 88 (2018) 162-171.
3. Z. Yilbaşi, M.K. Yesilyurt, M. Arslan, *Biomass Convers. Bior.,* (2021).
4. V. Brighenti, M. Protti, L. Anceschi, C. Zanardi, L. Mercolini, F. Pellati, *J. Pharm. Biomed. Anal.,* 192 (2021) 113633.
5. Á. Torrinha, S. Morais, *Trends Anal. Chem.,* 142 (2021) 116324.
6. A.M. Musa, J. Kiely, R. Luxton, K.C. Honeychurch, *Trends Anal. Chem.,* 139 (2021) 116254.
7. C.S. Ong, Q.H. Ng, S.C. Low, *Monatsh. Chem.,* 152 (2021) 705-723.
8. M. Pohanka, *Int. J. Electrochem. Sci.,* 15 (2020) 11024-11035.
9. G.J. Thangamani, K. Deshmukh, T. Kovářík, N.A. Nambiraj, D. Ponnamma, K.K. Sadasivuni, H.P.S.A. Khalil, S.K.K. Pasha, *Chemosphere,* 280 (2021) 130641.
10. J.M. Gonçalves, P.R. Martins, D.P. Rocha, T.A. Matias, M.S.S. Julião, R.A.A. Munoz, L. Angnes, *J. Mater. Chem. C,* 9 (2021) 8718-8745.
11. F.X. Wang, C.C. Wang, P. Wang, B.C. Xing, *Chinese J. Inorg. Chem.,* 33 (2017) 713-737.

12. X.Y. Zhao, W.L. Bai, Y.J. Yan, Y.F. Wang, J.K. Zhang, *J. Electrochem. Soc.,* 166 (2019) B873-B880.
13. W. He, X.Q. Li, Z.X. Qian, Z. Liu, Z.H. Tang, *Int. J. Electrochem. Sci.,* 14 (2019) 8781-8792.
14. A.B. Kanu, *J. Chromatogr. A,* 1654 (2021) 462444.
15. J. Marfà, R.R. Pupin, M.P.T. Sotomayor, M.I. Pividori, *Anal. Bioanal. Chem.,* (2021) 6141-6157.
16. Q. Wang, C. Gu, Y. Fu, L. Liu, Y. Xie, *Molecules,* 25 (2020) 4557.
17. Y. Fu, Z. You, A. Xiao, L. Liu, *Microchim. Acta,* 188 (2021) 71.
18. F. Yin, F. Xu, K. Zhang, M. Yuan, H. Cao, T. Ye, X. Wu, F. Xu, *Food Chem.,* 364 (2021) 130216.
19. Y. Zhang, Z. You, C. Hou, L. Liu, A. Xiao, *Nanomaterials,* 11 (2021) 2227.
20. Y. Cen, A.P. Xiao, X.Q. Chen, L.L. Liu, *J. Sep. Sci.,* 40 (2017) 4780-4787.
21. X. Yao, J. Shen, Q. Liu, H. Fa, M. Yang, C. Hou, *Anal. Methods,* 12 (2020) 4967-4976.
22. Z. You, Y. Fu, A. Xiao, L. Liu, S. Huang, *Arab. J. Chem.,* 14 (2021) 102990.
23. J. Ru, X. Wang, X. Cui, F. Wang, H. Ji, X. Du, X. Lu, *Talanta,* 234 (2021) 122679.
24. S.B. Kulkarni, U.M. Patil, I. Shackery, J.S. Sohn, S. Lee, B. Park, S. Jun, *J. Mater. Chem. A,* 2 (2014) 4989-4998.
25. L.L. Liu, Y.J. Ma, X.Q. Chen, X. Xiong, S.Y. Shi, *J. Chromatogr. B,* 887 (2012) 55-60.
26. J.C. Yang, J. Lee, S.W. Hong, J. Park, *Sens. Actuators B,* 320 (2020) 128366.
27. B. Tse Sum Bui, K. Haupt, *J. Mol. Recognit.,* 24 (2011) 1123-1129.
28. Y. Cui, J. Lin, Y. Xu, Q. Li, Y. Chen, L. Ding, *Sep. Purif. Technol.,* 276 (2021) 119302.
29. C. Zhong, B. Yang, X. Jiang, J. Li, *Crit. Rev. Anal. Chem.,* 48 (2018) 15-32.
30. T. Zhang, J.Z. Wei, X.J. Sun, X.J. Zhao, H.L. Tang, H. Yan, F.M. Zhang, *Inorg. Chem. Commun.,* 111 (2020) 107671.
31. S. Wu, Q. He, C. Tan, Y. Wang, H. Zhang, *Small,* 9 (2013) 1160-1172.
32. C. Akkapinyo, K. Subannajui, Y. Poo-arporn, R.P. Poo-arporn, *Molecules,* 26 (2021) 2312.
33. M. Sharafeldin, G.W. Bishop, S. Bhakta, A. El-Sawy, S.L. Suib, J.F. Rusling, *Biosens. Bioelectron.,* 91 (2017) 359-366.
34. Y. Poo-arporn, S. Pakapongpan, N. Chanlek, R.P. Poo-arporn, *Sens. Actuators B,* 284 (2019) 164-171.
35. B. Sun, X. Gou, R. Bai, A.A.A. Abdelmoaty, Y. Ma, X. Zheng, F. Hu, *Mat. Sci. Eng. C,* 74 (2017) 515-524.
36. M. Cirrincione, B. Zanfrognini, L. Pigani, M. Protti, L. Mercolini, C. Zanardi, *Analyst,* 146 (2021) 612-619.
37. D. López-Iglesias, J.J. García-Guzmán, C. Zanardi, J.M. Palacios-Santander, L. Cubillana-Aguilera, L. Pigani, *J. Electroanal. Chem.,* 878 (2020) 114591.
38. U. Backofen, F.-M. Matysik, C.E. Lunte, *J. Chromatogr. A,* 942 (2002) 259-269.
39. D. Duan, J. Ye, K. Li, *Sens. Actuators B,* 344 (2021) 130222.
40. N. Karuppusamy, V. Mariyappan, S.-M. Chen, M. Keerthi, R. Ramachandran, *Colloids Surf. A,* 626 (2021) 127094.
41. G. Mathew, P. Dey, R. Das, S.D. Chowdhury, M. Paul Das, P. Veluswamy, B. Neppolian, J. Das, *Biosens. Bioelectron.,* 115 (2018) 53-60.
42. Q. He, Y. Wu, Y. Tian, G. Li, J. Liu, P. Deng, D. Chen, *Nanomaterials,* 9 (2019) 115.
43. W. Liang, Y. Rong, L. Fan, C. Zhang, W. Dong, J. Li, J. Niu, C. Yang, S. Shuang, C. Dong, W.Y. Wong, *Microchim. Acta,* 186 (2019) 751.